JOURNAL OF MATERIALS SCIENCE **38** (2003) 995–1005

Comparative atmospheric corrosion of primary and cold rolled copper in Australia

J. D. NAIRN*, S. G. SKENNERTON, A. ATRENS
Department of Mining, Minerals and Materials Engineering, The University of Queensland, Brisbane, Queensland 4072, Australia
E-mail: jnairn@qcl.com.au

Atmospheric corrosion tests, according to ASTM G50, have been carried out in Queensland, Australia, at three different sites representing three different environmental conditions. A range of materials including primary copper (electrosheet) and electrolytic tough pitch (traditional cold rolled) copper have been exposed. Data is available for five exposure periods over a three year time span. X-Ray Diffraction has been used to determine the composition of the corrosion products. Corrosion rates have been determined for each material at each of the exposure sites and are compared with corrosion rates obtained from other long term atmospheric corrosion test programs. Primary copper sheet (electrosheet) behaves like traditionally produced cold rolled copper (C11000) sheet but with an increased corrosion rate. This difference between the rolled copper samples and the primary copper samples is probably due to a combination of factors related to the difference in crystallographic texture of the underlying copper, the morphology and texture of the cuprite layer, the surface roughness of the sheets, and the differences in mass. These factors combine together to provide an increased oxidation rate and TOW for the electrosheet material and which is significantly higher at the more "tropical" sites. For a sulfate environment (Urban) the initial corrosion product is cuprite with posnjakite and brochantite also occurring at longer exposures. Posnjakite is either "washed away" or converted to brochantite during further exposure. The amount of brochantite increases with exposure time and forms the blue-green patina layer. For a chloride environment (Marine) the initial corrosion product is cuprite with atacamite also occurring at longer exposures.

1. Introduction

Primary copper sheet was produced by electrolytic refining of copper anodes supplied through the smelting of copper ores (ISAPROCESS, Copper Refineries Limited, Townsville). This process is an innovative method to produce copper sheet without the need for the traditional metal processing steps of casting and cold rolling. The primary copper sheet (also known as "electrosheet") has a purity of 99.9+% and a thickness of 0.6 mm. This material conforms well with the traditionally specified copper roofing material of "16 ounce 110 cold rolled copper" (C11000, Electrolytic Tough Pitch Copper, 99.9% Cu, 0.04% O, 0.6 mm thick) and hence has been utilised in the installation of copper roofs. For this new material there was a requirement for the characterisation of material, as produced, and to assess its performance on subsequent atmospheric exposure. This requirement was met by comparative atmospheric corrosion testing of primary copper and copper produced by more traditional means (cold rolled), and this paper reports these results.

Atmospheric corrosion results are important because they represent the performance of real materials in real environments. Quantitative knowledge of the corrosion properties of a material specified to be exposed in a natural environment has long been recognised as valuable, if not essential, by material suppliers, architects and engineers [1].

Copper exposed to the atmosphere undergoes various stages of reaction from the time of installation to the development of the natural patina, which may take up to 50 years. Copper patinas are chemically and metallurgically complex structures and are produced by the chemical reaction of copper and trace elements in the atmosphere (particularly sulfate and chloride) [2–4]. Initially the copper has a bright orange metallic surface. After a few months the copper surface develops a uniform primary protective film of cuprite (Cu_2O), which has a matt brown colour and continues to darken with exposure. Subsequently, a second blue green layer forms on the surface of the cuprite. The colour of this patina layer depends on local atmospheric conditions.

*Author to whom all correspondence should be addressed.

Once the patina is established it is stable and copper corrosion occurs at an ever diminishing rate. The patinated copper typically consists of:

- The underlying copper metal (typically 99+ wt% Cu).
- A thin layer (5 to 20 um) of cuprite, Cu_2O.
- A top layer of basic copper sulfate (brochantite) or basic copper chloride (atacamite)

2. Experimental procedure

2.1. Atmospheric exposure

The atmospheric corrosion test followed the ASTM standard G50-76 for "Conducting Atmospheric Tests on Metals" [5]. Samples were exposed at three different sites in Queensland, Australia, representing three different corrosive environments: (1) University of Queensland (UQB), Brisbane, (Moderate); (2) Copper Refineries Ltd (CRL)., Townsville, (Industrial/ Tropical); and (3) CRL Shipping Port (PRT), Townsville. (Severe Marine/Tropical)

Testwork has proceeded for three years with samples removed five times during this time span (three months, six months, one year, two years and three years). Provision has been made to extend this testwork as copper roofs are expected to last many hundreds of years and hence atmospheric corrosion tests must span many years to provide credible results that can be used to predict the lifetime of the roofing material.

2.2. Material type and preparation

Three different forms of copper are being tested: "electrosheet" primary copper (as-received); "electrosheet" primary copper (acid cleaned); and traditional cold rolled copper (acid cleaned C11000).

Triplicate specimens of each material have been exposed for each time period. All specimens for testing were produced as 70 mm $\times$ 100 mm sheets with an identifying code stamped on the back of each sheet. Each of the as-received materials (electrosheet and traditional copper) were cleaned and de-greased to a "no water break" finish before further treatment or exposure. Each of the sample types were prepared in the following manner.

2.2.1. Electrosheet (ES)

Electrosheet was delivered as grease free sheets with a layer of purple copper oxide on one side. Cleaning of this sheet was performed in an ultrasonic cleaner using acetone. After cleaning the samples were thoroughly washed, rinsed in ethanol and dried. The samples were then weighed and stored (desiccator). The electrosheet had an average thickness of 0.65 mm and the specimens had an average weight of 39.6 g.

2.2.2. Electrosheet acid cleaned (EA)

Electrosheet samples to be acid cleaned were initially degreased using the acetone treatment and were then cleaned of oxide using the two stage acid treatment detailed in ASTM standard G1-90 for "Preparing, Cleaning and Evaluating Corrosion test specimens" [5]. The 10% sulfuric acid solution (C.2.3) was employed using an ultrasonic cleaner to decrease the treatment time. Much of the copper oxide present was reduced to copper by the acid and re-precipitated on the copper surface. Brushing removed most of this material and the second solution (12% sulfuric acid 0.3% sodium dichromate, C.2.4) removed the remaining precipitated copper producing a shiny clean surface. After cleaning the samples were washed, rinsed in ethanol, dried, weighed and stored. The average weight loss caused by acid cleaning was found to be 0.20 g.

2.2.3. Traditional copper (TC)

A material was chosen that was commonly available and was close to the copper electrosheet in composition: C11000, Electrolytic Tough Pitch copper (99.9% Cu). Atmospheric corrosion data for this material is also available for comparison from previous tests [6–16]. The copper was obtained as 0.98 mm sheets with an average weight of 60.9 g for each sample. The copper was degreased with a hot alkaline degreaser (to remove manufacturing greases and oils) and then acid cleaned using the sulfuric acid/ acidic dichromate solutions. After cleaning the samples were washed, rinsed in ethanol, dried, weighed and stored.

2.3. Materials characterisation

A small piece of each original material was placed in a Phillips X-Ray Diffractometer equipped with a Sietronics SIE122D Interface and scanned between 10 and 95° at a scan speed of 1°/minute using Cu K_α radiation produced from a X-Ray source operating at 40 kV and 40 mA. The uPDSM search/match program using the PDF 1998 database was employed to solve the pattern obtained. The original materials were also examined using a JOEL JSM-6400F field emission Scanning Electron Microscope (SEM) and the surface roughness was measured with a Taylor-Hobson SURTRONIC-3 with a 5 um tip radius diamond stylus. Metallographic cross-sections of each copper type were prepared by mounting in epoxy resin, polishing to a 1 μm diamond finish and etching in alcoholic ferric chloride.

All the cleaned and weighed copper specimens were installed on exposure racks (separated by porcelain insulators) at the three exposure sites. After exposure the samples were removed from the testing environment and analysed for corrosion rates and corrosion products. All exposed specimens were weighed after exposure (to determine weight gain due to oxidation). From each of the triplicate samples, two were acid cleaned (sulfuric acid/ acidic dichromate solutions) to remove the oxide and re-weighed to determine the corrosion rates while the third sample was kept for characterisation of the corroded surface. Characterisation of the corrosion products was accomplished using X-ray Diffraction (XRD).

3. Results

3.1. Original materials

Electrosheet (ES) was obtained with a layer of purple copper oxide on one side. X-Ray Diffraction revealed this layer to be mostly cuprite (Cu_2O) with

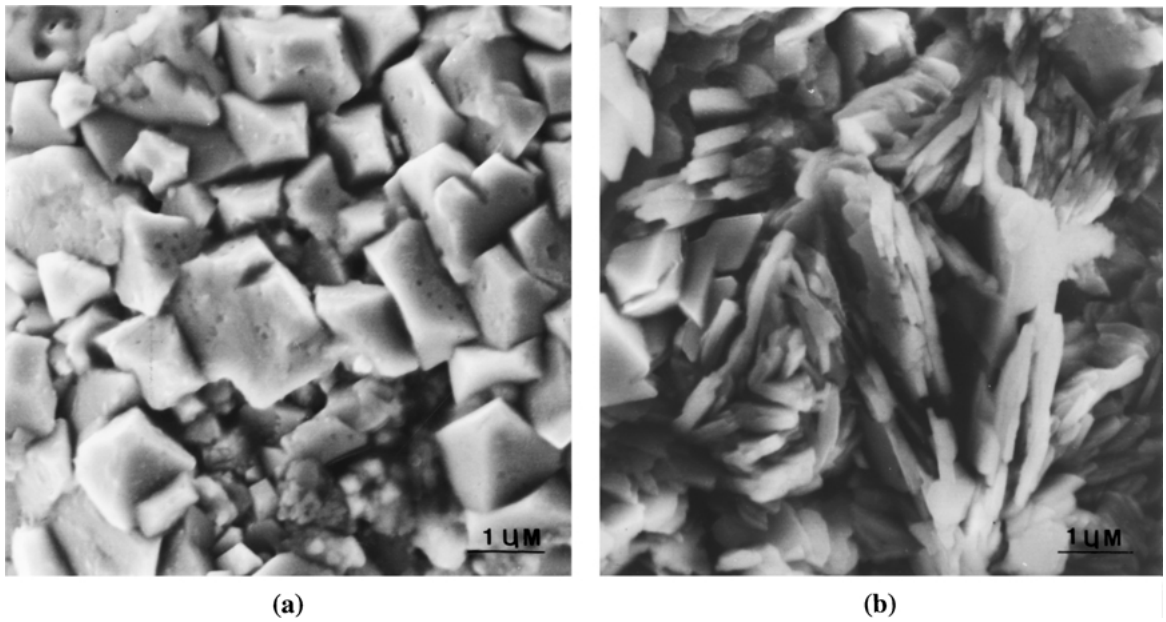

Figure 1 SEM image of Electrosheet surface showing the surface covered by (a) octahedral crystals of cuprite and (b) brochantite crystals growing over the cuprite layer.

a small amount of basic copper sulfates (e.g. brochantite, $3Cu(OH)_2 \cdot CuSO_4$) also present. The sulfates originated from small residues of electrolyte (acidic copper sulfate solution) that remained on the surface after washing of the freshly produced electrosheet. The oxide grew quickly after removal of the sheet from the electrolytic refining tank and reached a maximum thickness in about 4 weeks with the top surface having a thickness of about 4 um and with a 1 um thick film on the back of the electrosheet. The oxide consisted of a layer of octahedral cuprite crystals of about 1 um in diameter as shown in Fig. 1a. Brochantite also existed on the surface in very small amounts as crystals growing over the cuprite layer as shown in Fig. 1b. This brochantite was present as small agglomerations of individual facetted plates. This form of brochantite is not very adherent and was found to be removed after initial atmospheric exposure due to weathering. This is in contrast to the microcrystalline and adherent morphology that brochantite obtains during natural patination. The surface roughness of this material was $R_a = 1.10\ \mu$m. Acid cleaning of the electrosheet (EA) produced a material which had a slightly lowered surface roughness, $R_a = 0.98\ \mu$m, but with many surface irregularities and cavities as shown in Fig. 2a. Degreasing and acid-cleaning of the traditional copper (TC) produced a surface which was quite smooth, $R_a = 0.13\ \mu$m in the rolling direction and a $R_a = 0.15\ \mu$m across the rolling direction, and showed a more regular nature and an absence of cavities as shown in Fig. 2b.

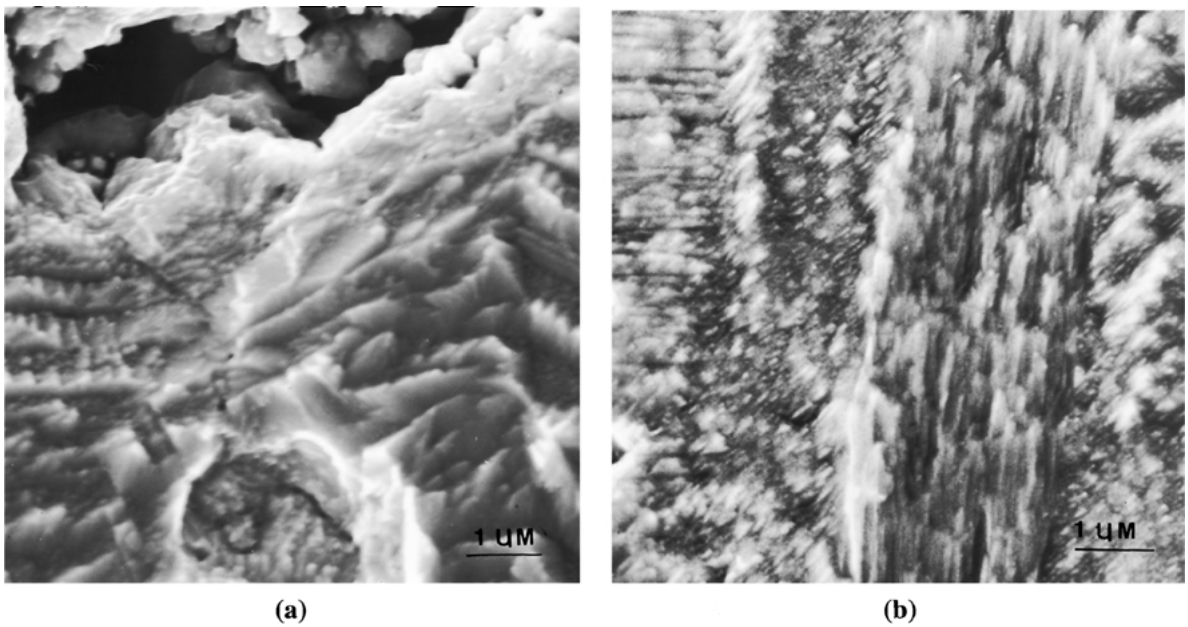

Figure 2 SEM image of (a) acid cleaned electrosheet revealing the granular structure, irregular surface and cavities of the etched copper surface and (b) the acid cleaned traditional cold rolled copper showing the etched copper surface and residual rolling features.

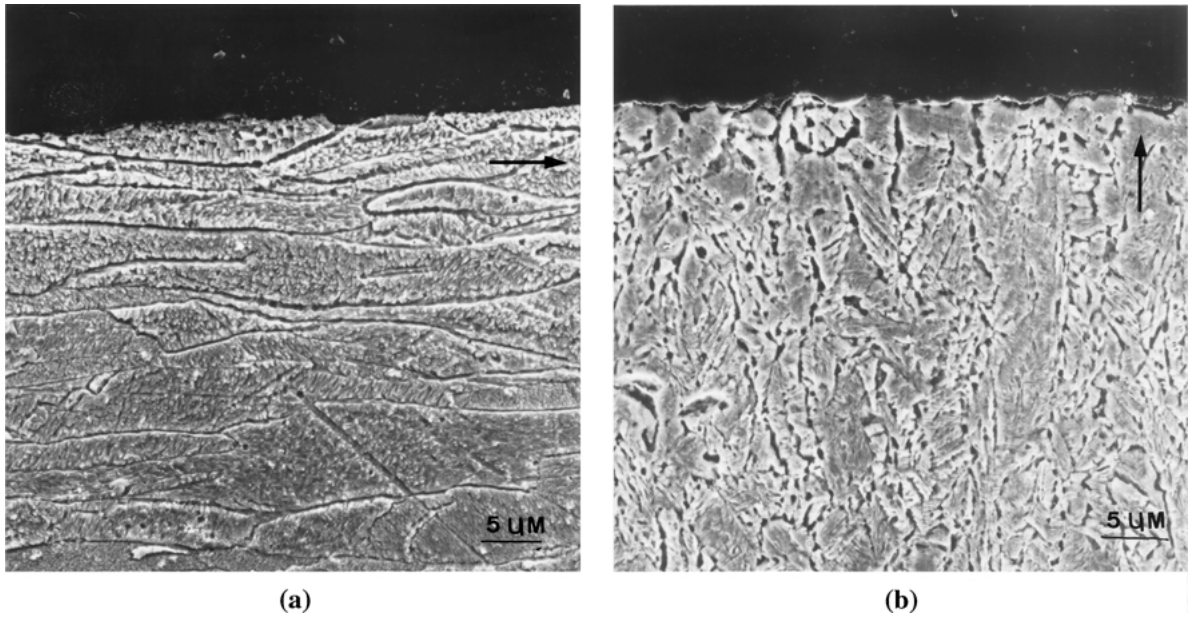

Figure 3 SEM image showing the polished and etched cross section of (a) traditional copper with the microstructure showing grains elongated in the direction of rolling (arrow) and (b) electrosheet showing twinned equiaxed grains with a slight columnar nature in the direction of growth (arrow).

Fig. 3a shows the microstructure of the traditional copper sheet which reveals a typical cold worked structure of grains elongated in the rolling direction (parallel to surface) while Fig. 3b reveals the electrosheet microstructure to consist of heavily twinned equiaxed grains showing a slight columnar nature in the direction of growth (perpendicular to surface). The nucleation and growth of copper crystals, from a hot acidic copper sulphate solution, onto a stainless steel sheet produced the electrosheet microstructure. The addition of special reagents and control of the anode dissolution and cathode growth conditions (electrode geometry, voltage, current, electrolyte composition and temperature) enabled the production of a copper sheet containing equiaxed grains rather than the columnar texture commonly found in electrolytic deposits. This resulted in the production of a high purity (due to smooth liquid/solid growth interface), flat and ductile copper sheet.

Due to the different methods of production for the copper sheets, XRD was employed to determine the differences in crystallographic texture for each. Fig. 4 shows the relative intensities of the individual copper crystal planes compared to the JCPDS [17] standard for Copper (4-0836). The results are presented in Table I and show that the electrosheet materials have a texture with the (100) and (110) planes showing an increase (when compared to the JCPDS 4-0836 standard) in relative amounts parallel to the sheets surface while the traditional copper has a texture with a very large increase in the amounts of (110) and (311) planes with a corresponding decrease in the presence of (111) and (100) planes. The texture revealed in the electrosheet is due to the equiaxed grains showing a slight texture in the growth direction. The texture in the traditional copper is due to the slip occurring along the (111) plane in the [110] direction during the cold rolling process that produces the elongated grains.

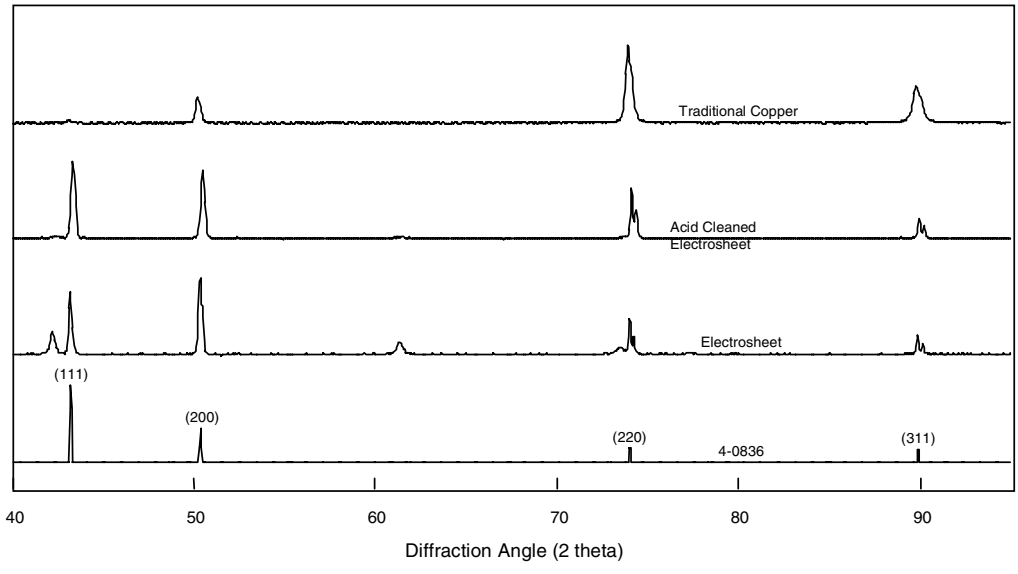

Figure 4 XRD scans of original materials showing their crystalline texture compared to the JCPDS standard for copper (4-0836).

TABLE I Relative XRD intensities for the individual copper crystal planes for the original copper materials (ES: Electrosheet. EA: Electrosheet Acid Cleaned. TC: Traditional Copper) and JCPDS standard for copper (4-0836)

	Relative XRD intensity		
Copper crystal face	JCPDS copper 4-0836	EA and ES	TC
(111)	100	80–100	3
(200)	46	80–100	33
(220)	20	30–60	100
(311)	17	20–30	48

3.2. Atmospheric corrosion testing results

The composition of the corrosion products for each material after each exposure period at each site was determined by XRD. Similar corrosion products were found on each of the different materials exposed at the same site for the same time period. The results are summarised in Table II. XRD scans for Electrosheet exposed at each of the sites for the five time periods are presented in Figs 5–7.

The cuprous oxide formed is nucleated epitaxially on the copper grains from adsorbed oxygen before growing laterally across the copper surface producing a layer consisting of an aggregate of individual grains orientated to the existing copper grains. Fig. 8 shows the relative intensities of the individual cuprite crystals that have formed on the electrosheet and traditional copper samples after three months exposure at the CRL site. The results are presented in Table III which shows that the oxide formed on the electrosheet shows very little difference to the JCPDS standard for cuprite (78-2076) while the oxide formed on the traditional copper has increased amounts of (110) planes due to the original highly textured cold rolled copper and orientation relationship between the original copper grains and the cuprite formed [18]. This oxide texture determined for each type of material was found to be the same at each site for all exposure periods. While there would be initial differences in the lateral growth of the oxide once the layer is continuous and thicker than 100 nm the continued growth of the oxide is governed by diffusion of ions and electrons through the oxide. Network modifying oxides such as cuprite grow by cation transport through the movement of cation vacancies (p-type semiconductor). For a cubic oxide, such as cuprite, diffusion rates of the cation vacancies should be independent of oxide orientation resulting in corrosion rates that are independent of oxide orientation. On the other hand, the electrosheet has a much finer grain size than the traditional cold rolled copper which would result in a cuprite layer with a larger number of single grains and a larger proportion of imperfections and grain boundaries which could result in increased diffusion and corrosion rates.

TABLE II Corrosion products detected by XRD on exposed copper samples

		Exposure time				
Exposure site	Relative amount of corrosion product	3 months	6 months	1 year	2 years	3 years
UQB, Brisbane (Moderate)	Major	Cuprite	Cuprite	Cuprite	Cuprite	Cuprite
	Minor	–	–	–	Posnjakite, Brochantite	Brochantite
	Trace	–	–	Posnjakite, Brochantite	–	–
CRL, T'ville (Industrial/Tropical)	Major	Cuprite	Cuprite	Cuprite	Cuprite	Cuprite
	Minor	Posnjakite	Posnjakite, Brochantite	Brochantite	Brochantite	Brochantite
	Trace	Brochantite	–	Posnjakite	–	–
PRT, T'ville (Severe Marine/Tropical)	Major	Cuprite	Cuprite	Cuprite	Cuprite	Cuprite
	Minor	–	–	Atacamite	Atacamite	Atacamite
	Trace	–	Atacamite	Posnjakite	Posnjakite	Posnjakite

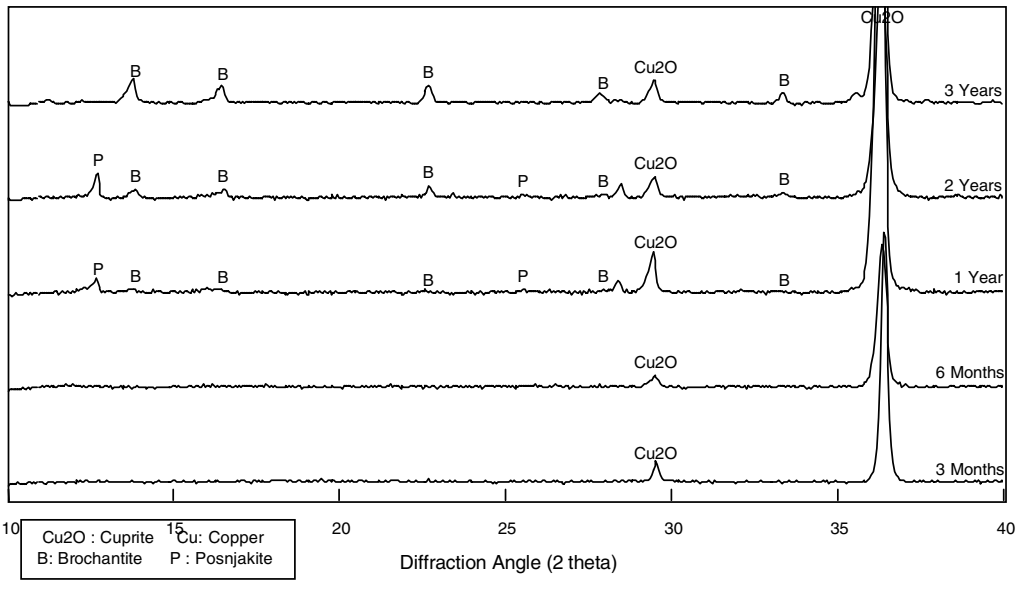

Figure 5 XRD scans for electrosheet exposed for up to 3 years at UQB, Brisbane.

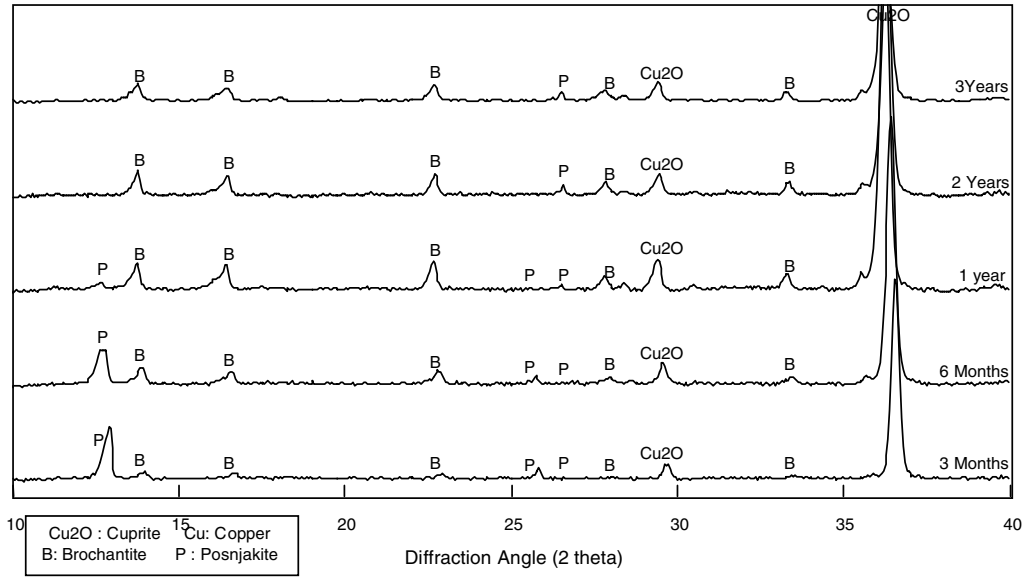

Figure 6 XRD scans for electrosheet exposed for up to 3 years at CRL, Townsville.

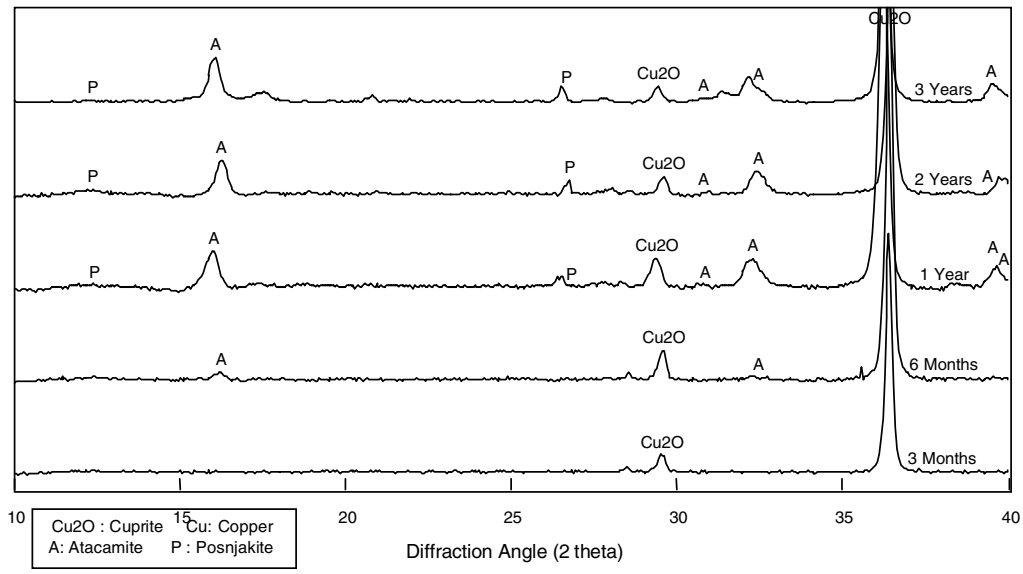

Figure 7 XRD scans for electrosheet exposed for up to 3 years exposure at the PRT, Townsville.

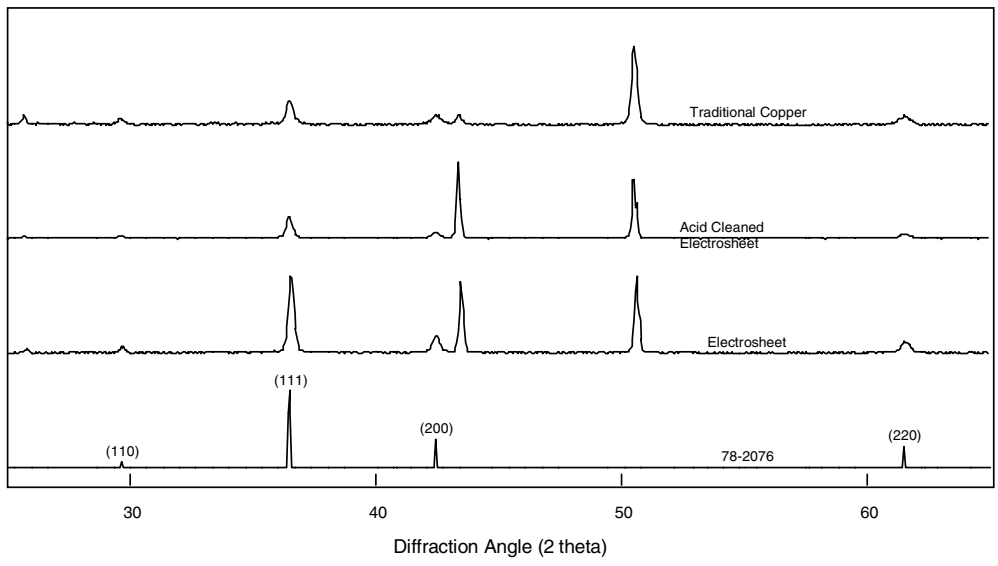

Figure 8 XRD scans for 3 months exposure at CRL site, Townsville, showing texture of the cuprite developed in comparison to the JCPDS standard for cuprite (78-2076).

TABLE III Relative XRD intensities for cuprite crystals on copper samples after three months exposure at the CRL site. (ES: Electrosheet. EA: Electrosheet Acid Cleaned. TC: Traditional Copper)

Cuprite crystal face	Orientation relationship Cu_2O/Cu	Relative XRD intensity		
		JCPDS Cuprite 78-2076	ES and EA	TC
(110)	(110)/(110)	5	7–10	20–30
(111)	(111)/(111)	100	100	100
	(111)/(100)			
(200)	(100)/(100)	35	20–25	20–30
(220)	(110)/(110)	27	15–20	30–40

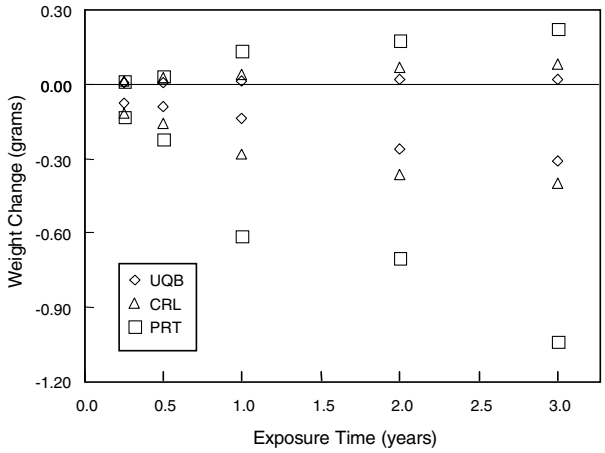

Figure 9 Weight change after exposure for electrosheet at the three exposure sites. (UQB: University of Queensland, Brisbane. CRL: Copper Refineries Ltd., Townsville. PRT: CRL Shipping Port, Townsville).

Typical weight changes after exposure are illustrated in Fig. 9, which shows the data for the electrosheet at the three sites. The small weight increases were due to the oxidation of the copper samples (measured immediately after exposure) while the weight losses were due to the amount of copper that reacts to form the corrosion products (measured after acid cleaning to remove the oxide). The weight losses can be simply converted into corrosion rates (μm/yr) by using the relationship

$$\text{Corrosion Rate } (\mu\text{m/yr}) = kW/STD \qquad (1)$$

where $k =$ constant (10 000), $W =$ weight loss (g), $S =$ specimen area (cm^2), $T =$ exposure time (years), $D =$ alloy density (g/cm^3).

Previous studies [19, 20] have shown that metals that form adherent oxides, such as copper, show atmospheric corrosion rates that vary with time according to

$$C = AT^n \qquad (2)$$

Where C is the mean corrosion after T years of exposure, A is the corrosion rate after the first year of exposure and n is an exponent which is less than one for metals that have decreasing corrosion rates with time. This relationship can be used to produce a linear bi-logarithmic law for atmospheric corrosion

$$\log C = \log A + n \log T \qquad (3)$$

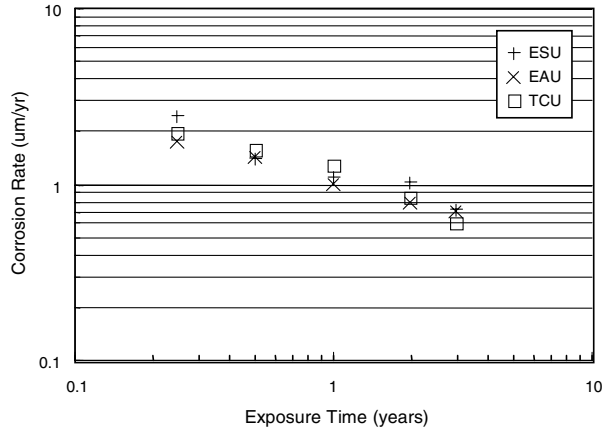

Figure 10 Atmospheric corrosion of copper at the UQB site (Brisbane) showing a linear bi-logarithmic law (ESU: Electrosheet, EAU: Electrosheet Acid Cleaned, TCU: Traditional Copper).

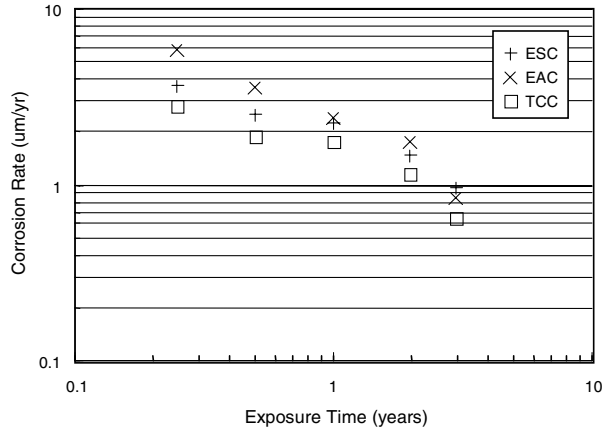

Figure 11 Atmospheric corrosion of copper at CRL site (Townsville) showing a linear bi-logarithmic law (ESC: Electrosheet, EAC: Electrosheet Acid Cleaned, TCC: Traditional Copper).

which shows that the corrosion behavior is governed by the parameters A and n. While A can be determined after one year of exposure n can only be reliably obtained after many years of exposure. The general nature of this law allows the prediction of long term corrosion behavior from relatively short exposure tests. Since a linear bi-logarithmic law for the atmospheric corrosion of copper is expected then a bi-logarithmic relationship should exist between mean corrosion rate and exposure time according to

$$\log C/T = \log A + (n-1) \log T \qquad (4)$$

Figs 10–12 show the expected bi-logarithmic relationship with corrosion rate decreasing with time for the UQB, CRL and PRT sites respectively.

4. Discussion

4.1. University of Queensland site

This site (UQB) in Brisbane, Queensland, is characterised by moderate rainfall (around 1000 mm p.a.), average daily humidity of 60%RH ($TOW_{80\%} = 27\%$, ISO category T3), average daily temperatures between 15°C and 25°C, some industrial pollution resulting in

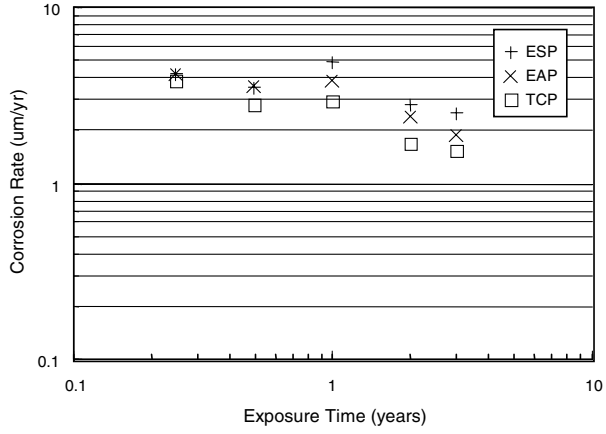

Figure 12 Atmospheric corrosion of copper at the PRT site (Townsville) showing a linear bi-logarithmic law (ESP: Electrosheet, EAP: Electrosheet Acid Cleaned, TCP: Traditional Copper).

a 0.002 ppm SO_2 level (SO_2 deposition of 4.43 mg m^{-2} day^{-1}, ISO category P0) [21] and is further than 15 km from the coastline. This corresponds to the Moderate (ISO Category 2) environmental category outlined in AS 2312 (1994) [22]. This environment is expected to result in a very low corrosion rate for the materials tested. This is supported by the results obtained (Fig. 10) with the materials tested showing an average corrosion rate at three years of about 0.7 μm/yr. The three materials tested showed very similar corrosion rates despite the difference in the initial surface conditions (roughness, oxide film) and copper microstructure (electrolytic, cold rolled).

The one year exposure corrosion rates are higher than expected based on the previous shorter term exposure samples but correlate well with the two and three year exposure corrosion rates. This is also more evident with the CRL and PRT site (Figs 11 and 12). This is common with materials exposed for less than one year and is attributed to seasonal variations of environmental factors [23]. The east coast of Australia experiences a very dry winter period followed by a hot, humid and rainy summer. In Brisbane, during summer, the temperature increases by an average of ten degrees, the rainfall increases from about 60 mm per month to 150 mm per month (with the number of rainy days increasing from 7 to 12 per month), and the average daily humidity increases from about 57% to 63%. Corrosion rates during the summer period are thus expected to be significantly higher than for the rest of the year. The testwork was commenced in May with the first two sets of samples removed during the winter and spring months. In comparison the one year samples also experienced the typical hot and wet summer resulting in the measured increased corrosion rate. Due to this seasonal variation extrapolation of the existing data, to determine the parameters A and n, was performed using only the 1, 2 and 3 year exposure data.

XRD results (Table II, Fig. 5) showed cuprite to be the initial corrosion product with a small amount of posnjakite and then some brochantite occurring at the later stages. Posnjakite is a hydrated form of brochantite and has been identified in short term exposures by previous researchers [3, 23–25]. The amount of brochantite formed appears to increase linearly with exposure time while the posnjakite reaches a maximum at about 2 years exposure and is absent after three years exposure. The posnjakite formed initially either dissolves at later stages or is converted to insoluble brochantite. This is supported by other researchers [3] who found decreasing amounts of posnjakite with time. Examinations of copper roof samples [8] (7 to 100 years) obtained from the Brisbane environment also reveal, by XRD, to contain no trace of posnjakite in their patinas but increasing amounts of brochantite with age.

Extrapolation of the corrosion results (Fig. 10) to 10 years exposure revealed an expected mean corrosion rate of about 0.4 μm/yr ($A = 1.15$, $n = 0.54$) for all materials tested. Even if no further decrease in corrosion rate occurs then a 0.6 mm thick copper roofing panel should not fail by uniform corrosion for at least 1000 years in the Brisbane environment.

4.2. Copper Refineries Limited, Townsville

This site in Townsville is located within the Copper Refineries Limited complex next to the Electrolyte Purification Plant (EPP) and is about 5 km from the coastline. The area is polluted by a fine aerosol carrying the acidic copper sulfate solution used in the electrorefining of copper. Combined with the high rainfall (>1200 mm p.a.), average daily temperatures between 20°C to 28°C and average daily relative humidity of 65%RH present this pollution makes this site very aggressive with nearby steelwork showing severe corrosion damage. This corresponds to the Industrial/Tropical (ISO Category 3) environmental category outlined in AS 2312 (1994) [22]. No measurement of the SO_2 deposition rate was performed but if the relative amounts of brochantite, determined by XRD, formed on the CRL site samples are compared to the UQB samples then it can be estimated that the SO_2 deposition rate at CRL is about 4 times higher than at UQB (SO_2 deposition of about 18 mg m^{-2} day^{-1}, ISO category P1). The high humidities and high rainfall are expected to place this environment in the ISO category T4.

The corrosion rates measured are higher (Fig. 11) than in Brisbane (UQB) with an average corrosion rate after three years of 0.8 um/yr. This increase in corrosion rate is expected and is due to the increased TOW, increased temperature and the increased pollution level (SO_2 deposition). Previous researchers [19] have found, by correlating data on pure copper from forty nine exposure sites, that the corrosion of copper was highly correlated with RH% and temperature.

The seasonal variation in corrosion found in Brisbane is also evident at this site with the one, two and three year exposure corrosion rates higher than expected based on the previous shorter term exposure samples. In Townsville, in summer, the temperature increases by an average of eight degrees, the rainfall increases from about 25 mm per month to 230 mm per month (with the number of rainy days increasing from 3 to 11 per month), and the average daily humidity increases from about 60% to 70%. Corrosion rates

during the summer period are thus expected to be significantly higher than for the rest of the year. Due to this seasonal variation extrapolation of the existing data, to determine the parameters A and n, was performed using only the 1, 2 and 3 year exposure data.

XRD results (Table II, Fig. 6) showed cuprite to be the initial major product formed with some posnjakite and a small amount of brochantite also occurring on the three month samples. The amount of brochantite continues to increase with the posnjakite amount decreasing to only a trace after two years exposure. This initial formation and disappearance of posnjakite is similar to that experienced at the UQB site but the amount of brochantite formed is much greater. Brochantite forms by the oxidation of cuprite with the protective film of cuprite being progressively covered by an adherent, but not protective (porous), brochantite layer. This results in a higher corrosion rate for the exposure sites with increased levels of pollutants such as SO_2 or chloride (e.g. CRL and PRT sites).

The measured corrosion rate for the traditional copper (C11000 copper) is consistently lower than the corrosion rates for the electrosheet and acid cleaned electrosheet. This difference between the rolled copper samples and the primary copper samples is probably due to a combination of factors related to the difference in crystallographic texture of the underlying copper, the morphology and texture of the cuprite layer, the surface roughness of the sheets, and the differences in individual sample mass.

Oxidation rate studies of single crystals of copper [18] have shown that the crystal face (100) has a higher rate of oxidation than the (110) face. Tables I and III respectively show the texture of the copper and cuprite for each of the materials being tested. The electrosheet has a crystallographic texture resulting in a higher proportion of (100) crystal faces on the surface while the traditional rolled copper has a crystallographic texture resulting in an increased proportion of (110) crystal faces on the surface. Thus the electrosheet is expected to experience a higher corrosion rate. This increased oxidation rate for the (100) faces is expected to be due to the different oxide orientations possible, (111) or (100), and therefore the increase in the number of imperfections and grain boundaries. In a similar way, the smaller grain size of the electrosheet will result in smaller cuprite crystals and therefore a protective film with an increased number of imperfections and grain boundaries compared to the traditional rolled copper sheet.

An increased "Time of Wetness" (TOW) could also be experienced by the primary copper (electrosheet) at this site due to its higher surface roughness and lower mass. The high surface roughness could lead to decreased critical relative humidities (longer TOW) due to capillarity effects while electrosheet samples, with their smaller individual sample weights (39.6 g), would cool quicker than the thicker traditional rolled copper samples (60.9 g) resulting in dew forming earlier and more readily on these samples. A metal panel located outdoors (exposure rack) will radiate heat at night to the cold sky thus becoming colder than the surrounding ambient air and resulting in condensation on the surface at ambient relative humidities below 100%. This temperature difference will depend upon the orientation of the sample to the sky, the thermal mass of the sample, and the surface-to-air heat transfer coefficient (wind velocity) [26]. Townsville experiences both high daytime temperatures and humidities resulting in nightfall condensation being common. It is quite likely that the thinner electrosheet experience longer TOW due to increased and more frequent condensation periods. This environmental effect would also explain the fact that the UQB site, which does not experience the high daytime temperatures and humidities and thus nightfall condensation, does not show any significant difference between the three materials tested while the CRT and PRT sites do even though the copper and cuprite morphologies and textures would be the same on each type of material at each site.

Extrapolation of the corrosion results (Fig. 11) to 10 years exposure reveals an expected mean corrosion rate for the electrosheet of about 0.4 μm/yr ($A = 2.35$, $n = 0.23$) while the traditional copper has an expected corrosion rate of 0.3 μm/yr ($A = 1.80$, $n = 0.22$).

4.3. Marine Port, Townsville

This site (PRT) is situated at a shipping port in Townsville about 50 m from the sea. The site experiences the same weather conditions (rainfall, temperature, and humidity) as the CRL site but it also experiences a high chloride deposition rate. This corresponds to the Severe Marine/Tropical (ISO Category 4) environmental category outlined in AS 2312 (1994) [22]. The corrosion rates are shown in Fig. 12.

Corrosion rates at this site are the highest for the three sites with an average corrosion rate at three years of 1.9 um/yr. This increase in corrosion rate is again expected to be due to the increased TOW, increased temperature and increased pollution level from the deposition of chloride salts.

It can be seen that the corrosion rates also decrease with time in a trend similar to those at the UQB and CRL sites and that the one year data is higher than the shorter term exposures. This again is due to the seasonal variations and their effect on short term corrosion rates. Due to this seasonal variation extrapolation of the existing data, to determine the parameters A and n, was performed using only the 1, 2 and 3 year exposure data.

XRD results (Fig. 7) show cuprite to be the initial corrosion product formed with basic copper chloride (atacamite) possibly occurring at longer exposures. Atacamite ($3Cu(OH)_2 \cdot CuCl_2$) is the expected patina compound that forms in a marine environment where the chloride concentration is much higher than the sulfate concentration [14]. Paratacamite, a polymorphic compound, is also commonly observed with copper exposed to chlorides and can be difficult to distinguish from atacamite particularly in specimens that have only been exposed for a short time, producing a small amount of the compound, and revealing only a few XRD peaks common to both compounds. At two years exposure the

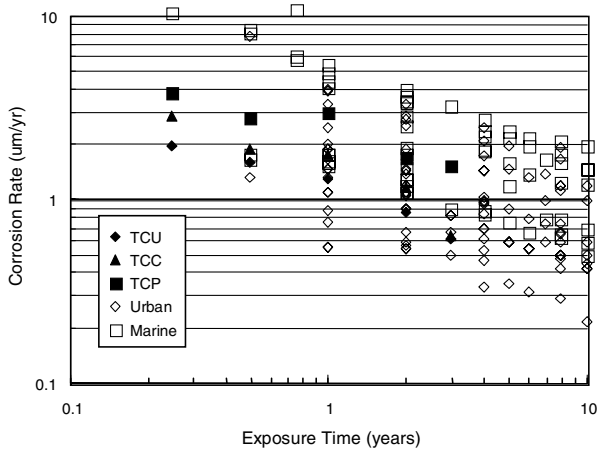

Figure 13 Comparison of atmospheric corrosion rates determined with data from other testing programs. (TCU: Traditional Copper, UQB site. TCC: Traditional Copper, CRL site. TCP: Traditional Copper, PRT site. Urban: literature data from sulfate polluted sites. Marine: literature data from chloride polluted sites).

amount of atacamite formed can be seen on the surface of the specimens as fine green spots.

Extrapolation of the corrosion results (Fig. 12) to 10 years exposure reveals an expected mean corrosion rate for the electrosheet of about 1.0 μm/yr ($A = 4.42$, $n = 0.35$) while the traditional copper has an expected corrosion rate of 0.6 μm/yr ($A = 3.00$, $n = 0.30$).

4.4. Comparison with previous testing programs

A number of long term atmospheric test programs have reported quantitative results on the atmospheric corrosion of copper at various sites [6–16]. Each of these environments investigated can be either classed as "Urban" or "Marine" depending on whether the predominant atmosphere pollutant is sulfate or chloride respectively. All literature results obtained have been plotted together with the corrosion rates determined from this program at each site for the traditional cold rolled copper (Fig. 13). This reveals that the corrosion rate of pure copper follows a bi-logarithmic function with the corrosion rate decreasing continuously with time.

Samples exposed at "Marine" environments show on average higher corrosion rates than samples exposed at "Urban" sites. Results from the present investigation for the traditional cold rolled copper fit well within the band of previous testwork results indicating that our testing procedures are valid. The electrosheet results are also quite similar to the traditional cold rolled copper (with a slightly increased corrosion rate) and shows that the electrosheet is behaving like traditionally specified "110" copper.

5. Conclusions

The microstructure of electrosheet consists of twinned equiaxed grains that show a significant texture difference to the elongated grains found in the traditional cold rolled copper. The cuprite formed is nucleated epitaxially on the copper grains forming a layer consisting of an aggregate of individual grains orientated to the existing copper grains. Atmospheric corrosion of "pure" copper alloys follow a bi-logarithmic function with corrosion rate decreasing with time and with primary copper sheet (electrosheet) behaving like traditionally produced cold rolled copper (C11000) sheet but with an increased corrosion rate. This difference between the rolled copper samples and the primary copper samples is probably due to a combination of factors related to the difference in crystallographic texture of the underlying copper, the morphology and texture of the cuprite layer, the surface roughness of the sheets, and the differences in mass. These factors combine together to provide an increased oxidation rate and TOW for the electrosheet material and which is significantly higher at the more "tropical" sites. For a sulfate environment (Urban) the initial corrosion product is cuprite with posnjakite and brochantite also occurring at longer exposures. Posnjakite is either "washed away" or converted to brochantite during further exposure. The amount of brochantite increases with exposure time and forms the blue-green patina layer. For a chloride environment (Marine) the initial corrosion product is cuprite with atacamite also occurring at longer exposures.

References

1. S. W. DEAN, "Atmospheric Corrosion" Hollywood, 1980 (1982) p. 195.
2. T. E. GRAEDEL, K. NASSAU and J. P. FRANEY, *Corrosion Science* **27** (1987) 639.
3. J. P. FRANEY and M. P. DAVIES, *ibid.* **27** (1987) 659.
4. K. NASSAU, P.K. GALLAGHER, A. E. MILLER and T. E. GRAEDEL, *ibid.* **27** (1987) 669.
5. Annual Book of ASTM standards, 03.02 (1994).
6. E. MATTSSON and R. HOLM, ASTM STP 435 (1968) p. 187.
7. M. MORCILLO, S. FELIU and S. GIMENEZ, Proceedings of the 10th International Congress on Metallic Corrosion, India 1987, *Key Eng. Materials* **20–28** (1988) 17.
8. J. D. NAIRN and A. ATRENS, *Materials Research 96,* IMMA, Brisbane, Australia (1996).
9. A. W. TRACY, ASTM STP 175 (1956) p. 67.
10. L. P. COSTAS, ASTM STP 767 (1982) p. 106.
11. A. P. CASTILLO and J. M. POPPLEWELL, ASTM STP 767 (1982) p. 60.
12. E. MATTSSON and R. HOLM, "Atmospheric Corrosion" Hollywood, 1980 (1982) p. 365.
13. V. KUCERA, D. KNOTKOVA, J. GULLMAN and P. HOLLER, Proceedings of the 10th International Congress on Metallic Corrosion, India 1987, *Key Eng. Materials* **20–28** (1988) 167.
14. L. VELEVA, P. QUINTANO, R. RAMANAUSKAS, R. POMES and L. MALDONADO, *Electrochimica Acta* **41** (1996) 1641.
15. G. SKENNERTON, J. NAIRN and A. ATRENS, *J. Mater. Lett.* **30** (1997) 141.
16. E. A. TAQI, *British Corrosion Journal* **29** (1994) 75.
17. JCPDS, International Centre for Diffraction Data, USA (1998).
18. A. RÖNNQUIST and H. FISCHMEISTER, *Journal of the Institute of Metals* **89** (1961) 65.
19. S. FELIU, M. MORCILLO and S. FELIU JR, *Corrosion Science* **34** (1993) 415.
20. M. POURBAIX, "Atmospheric Corrosion" Hollywood, 1980 (1982) p. 107.
21. D. KNOTKOVA, P. BOSCHEK and K. KREISLOVA, Atmospheric Corrosion ASTM STP 1239 (1995) p. 39.
22. AS2312, Guide to the Protection of Iron and Steel Against Exterior Atmospheric Corrosion (1994).
23. I. ODNEVALL WALLINDER and C. LEYGRAF, *Corrosion Science* **43** (2001) 2379.

24. I. ODNEVALL WALLINDER and C. LEYGRAF, *Journal Electrochemical Society* **142** (1995) 3682.
25. I. ODNEVALL WALLINDER and C. LEYGRAF, *Corrosion Science* **39** (1997) 2039.
26. P. GROSSMAN, Atmospheric Factors Affecting the Corrosion of Engineering Metals, ASTM STP 646 (1978) 5–16.
27. K. P. FITZGERALD, J. NAIRN and A. ATRENS, *Corrosion Science* **40** (1998) 2029.
28. A. R. MENDOZA and F. CORVO, *ibid.* **42** (2000) 1123.
29. W. HE, I. ODNEVALL WALLINDER and C. LEYGRAF, *ibid.* **43** (2001) 127.

Received 21 January
and accepted 5 November 2002